Hindawi
Journal of Robotics
Volume 2020, Article ID 8861847, 12 pages
https://doi.org/10.1155/2020/8861847

Research Article

Cascaded Control of Flexible-Joint Robots Based on Sliding-Mode Estimator Approach

Genliang Xiong,[1] **Jingxin Shi**,[2] **and Haichu Chen**[1]

[1]*School of Mechanical Engineering, Nanchang University, Nanchang XF999, China*
[2]*TTTech Germany GmbH, Shanghai 200070, China*

Correspondence should be addressed to Genliang Xiong; xionggenliang@ncu.edu.cn

Received 7 July 2020; Revised 22 September 2020; Accepted 30 September 2020; Published 27 October 2020

Academic Editor: Arturo Buscarino

The inherent highly nonlinear coupling and system uncertainties make the controller design for a flexible-joint robot extremely difficult. The goal of the control of any robotic system is to achieve high bandwidth, high accuracy of trajectory tracking, and high robustness, whereby the high bandwidth for flexible-joint robot is the most challenging issue. This paper is dedicated to design such a link position controller with high bandwidth based on sliding-mode technique. Then, two control approaches ((1) extended-regular-form approach and (2) the cascaded control structure based on the sliding-mode estimator approach) are presented for the link position tracking control of flexible-joint robot, considering the dynamics of AC-motors in robot joints, and compared with the singular perturbation approach. These two-link position controllers are tested and verified by the simulation studies with different reference trajectories and under different joint stiffness.

1. Introduction

The development of robotics in the past few years has been extended from the earlier standard applications of industrial robots to new fields such as space, service robotics, medical, and force-feedback systems. This demand makes the research directions on manipulators is to lighten the total weight while keeping the control and operation performance unchanged. Especially, desire for higher performance from the structure and mechanical specifications of chain-like mechanical manipulators has spurred designers to come up with flexible-joint robots. The topic of control of flexible-joint robots has troubled control experts of the world several decades.

Most of the researchers start the control design for flexible-joint robots with the Spong model [1]. Since then, a large amount of theoretical and experimental results are developed.

Some descriptions about the state-space approach based on the feedback linearization have been given before. As proposed by Spong in [2], even using a simplified robot model (i.e., the joint flexibility is generated by linear spring and the kinetic energy of a joint is only generated by the rotation of this joint), the resulting control algorithm is rather complicated, due to the state transformation and the inverse calculation of the control input. The control algorithm depends on the robot parameters, which are generally unknown. The robust analysis about the feedback linearization approach can be found in [3].

In general case of the flexible-joint robot model, the static feedback linearization may not be realizable [4]. De Luca and Lucibello involve the previous system information to form the so-called dynamic feedback linearization [5]. He uses not only the actual states of the robot, but also the past states; no global state transformation is required. The resulting control structure is of $2n(n-1)$ order (with n being the number of robot joints). He pointed out the sufficient condition of dynamic feedback linearization: there is no zero dynamics in the system. The authors in [5] won a best paper award during conference IRCA98 due to the theoretical contribution. For a simplified flexible-joint robot model, both static and dynamic feedback linearization can

be applied. However, both linearization methods need the state variables which may not be measured in a practical robot system. An observer design for the unmeasured state variables has been proposed [6, 7]. However, these observer design approaches increased the complexity of the control system and may make the feedback linearization meaningless.

Singular perturbation approach is one of the promising approaches to control the real-world lightweight robots, which solves the control problem in two time scalars: a fast joint torque control (often in form of a damping) term for the fast mode of the joint torque dynamics, and a slow joint torque feedforward term for the outer position control loop (related to the rigid-body dynamics of the robot arm) [8]. More about the research works of singular perturbation approach for flexible-joint robots can be found in [9–12].

Integral back-stepping approach is actually one of the pure cascaded control approaches and has the advantages such as not sensitive to the joint stiffness; state variables used for the control implementation are available. It provides a systematic way, i.e., a step-by-step way to design a Lyapunov function for the overall control system. However, the resulting controllers based on the basic version of integral back-stepping approach need system parameters; thus, the approach is sensitive to these parameters. To overcome this drawback, the Lyapunov function is often extended to involve a parameter adaptation process and the system robustness with respect to the parameter variations is theoretically ensured. However, the parameter adaptation process makes the overall control system more complicated and may not be able to react on the fast changing of the system parameters. Therefore, integral back-stepping approach provides more theoretical contribution than it practically does. Some works about the integral back-stepping approach used for the control of flexible-joints robots can be found in [13, 14].

Passivity-based control approach uses the concept of storage energy as well as storage energy changing (in time), providing a sufficient condition for a dynamic system to be stable. This control approach possesses some nice features: physically interpretable, systematical Lyapunov stability proof (using just the energy functions of the system), certain degree of robustness with respect to system uncertainties, simple-form controller, applicable to the case when contacting with environmental objects, etc. The author believes that passivity-based control approach is another promising control approach besides the singular perturbation approach. Ott studied the passivity-based control approach for flexible-joint robots systematically and showed the potential of this approach for different control tasks [15]. From the work of Ott, it seems that the only weak point of this control approach lies in the tracking control performance; this might be the price one has to pay for the nice features. Other research works about the passivity-based control approach used for the control of flexible-joint robots can be found in [16, 17]. In the literature about the passivity-based control approach for flexible-joint robots, the dynamics of the electric motor used in the robot joint were generally and unfortunately not taken into account.

It is clear that the advance control approaches for flexible-joint robots need the support of advance control theories. However, it seems that the model-based control theories in the last 20 years have not got significant progress in the sense of solving real-world control problems, such as the control of flexible-joint robots as high-order, nonlinear, uncertain MIMO systems. On the other hand, non-model-based control approaches such as fuzzy-logic control and neutral network-based control have been tested everywhere and it is hoped that these control approaches are universal and applicable to any dynamic system. However, the value of non-model-based control approaches is often over estimated. As mentioned before, the non-model-based control approaches may not be applicable to the control of high-order systems. The above observations have motivated researchers to find a middle way between model-based and non-model-based control designs. It is recognized, meanwhile, that to design a good control system, the controller designer has to possess a deep understanding about the physic plant to be controlled, independent of which control approach is applied. As a result, for control engineers who have no "good feeling" about the controlled plant, a rough model which contains the basic bone structure of the dynamic system is highly desirable, though there are some unmodeled dynamics, external disturbances, and parameter uncertainties associated with this rough model. As a candidate of the control theories which are able to handle the basic bone-structure model with a high degree of robustness, variable structure control as well as sliding-mode control [18] (in this thesis, no difference is made between these two closely related control approaches) has been selected for the control problems of the uncertain nonlinear systems [19–22]. It well known that sliding-mode control theory can be applied to high-order, nonlinear, uncertain MIMO systems and the resulting controllers are generally simple enough for the real-time implementation. Another advantage of sliding-mode control theory is easy to understand for "normal" control engineers. The major disadvantage associated with sliding-mode control is the chattering phenomena due to the high-frequency switching of the discontinuous control input. However, if the chattering problem can be solved or the inherent discontinuous property of the final control inputs (for the case of flexible-joint robots, the final control inputs are the terminal voltages on the stator windings of the electric motor used in robot joints) can be positive utilized, sliding-mode control theory will be a good control design tool for the systems such as flexible-joint robots.

Besides using the control approaches discussed above, adaptive control techniques [23], fuzzy logic and neural network approaches [24], and simple PD (or PID) control [25] were also used to the control of flexible-joint robots.

If selecting the link position and the joint torque as state variables, the Spong model can be transformed into the block form of state-space description as follows:

$$\begin{cases} M(q)\ddot{q} + C(q,\dot{q})\dot{q} + G(q) + F(\dot{q}) = \tau, \\ \ddot{\tau} + A_{\tau}(t)\tau + D_{\tau}(t) = B_{\tau}\tau_{m}, \end{cases} \tag{1}$$

where $M(q) \in \mathfrak{R}^{n\times n}$is the mass matrix, $C(q,\dot{q})\dot{q} \in \mathfrak{R}^n$is the vector including centrifugal and Coriolis forces, $G(q) \in \mathfrak{R}^n$is the gravity force vector, $F(\dot{q}) \in \mathfrak{R}^n$is the friction force vector, $q \in \mathfrak{R}^n$is the link position vector, $\tau \in \mathfrak{R}^n$is the joint torque vector $A_\tau(t) = K(J^{-1} + M\ (q)^{-1}), D_\tau\ (t) = K(J^{-1}\tau_{ds} + M(q)^{-1}N(q,\dot{q})), B_\tau = K\Gamma, N(q,\dot{q}) = C(q,\dot{q})\dot{q} + G(q) + F(\dot{q})$, $\tau_m \in \mathfrak{R}^n$ is the motor torque vector, $\tau_{ds} \in \mathfrak{R}^n$is the disturbance torque vector, $J = [J_i] \in \mathfrak{R}^{n\times n}$is the diagonal joint inertia matrix, $K = [k_i] \in \mathfrak{R}^{n\times n}$is the diagonal joint stiffness matrix, and $\Gamma = [\gamma_i] \in \mathfrak{R}^{n\times n}$is the diagonal gear-ratio matrix.

Equation (1) is actually a two-block system, block A and block B, as shown in Figure 1. The motor torque τ_m generates the joint torque τ, while the joint torque τ generates the motion of the link position q. In the joint torque dynamics, i.e., the second equation of (1), the influence of the link position and its time derivative exists. Normally, this influence is treated as system uncertainties when designing the joint torque controller, because the model parameters are generally unknown.

It is recognized that the dynamics of block B should be faster than the ones of block A, otherwise it makes no sense. This assumption is true for all designed robot manipulators so far, regardless of how large compliance the robot joints have. For this two-block system, many control approaches have been developed for the problem of link position control, either trajectory tracking control or point-to-point regulation.

The basic problems of the existing control approaches can be summarized as follows:

(1) The dynamics of the electric motor are generally not considered. In the literature, some researchers considered the motor dynamics (most of them used only a DC-motor model instead of an AC one), but the physical properties of the electric motor were not positively utilized to increase the system performance. Instead, the motor dynamics was always as negative effect taken into account.

(2) The existing control approaches generally lack joint torque tracking control capability. Some of the control approaches do not take joint torque as a state variable (or called interface variable) to be controlled; thus, the extension to the end-effect force and impedance control is not straightforward.

(3) Link position tracking control, joint torque tracking control, dynamics of AC-motors, and robustness with respect to the system uncertainties were not considered simultaneously.

In this paper, we will consider all aspects in point (3) simultaneously. As first, we add the motor dynamics to form the so-called three-block formulation of flexible-joint robots as shown in Figure 2.

As mentioned before, the dynamics of block B are faster than the ones of block A. However, the dynamics of block B may be faster or slower than the ones of block C (i.e., the dynamics about the motor currents). If the dynamics of block B are faster than that of block C, for the joint torque tracking control, a cascaded control structure with an inner current control loop and an outer joint torque control loop would not work properly. Therefore, we need a general solution to control the joint torque, independent of which block is faster among blocks B and C. Such a joint torque control approach has been presented in [26].

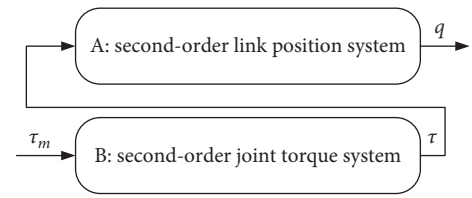

Figure 1: Two-block system of flexible-joint robots.

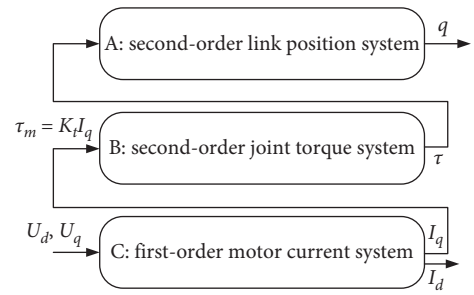

Figure 2: Three-block system of flexible-joint robots.

For the link position control issues discussed in this paper, two control approaches will be presented. In Section 2, we review the singular perturbation approach to work with the robust link position controller for rigid-body manipulators and with the direct sliding-mode current control. In Section 3, we integrate the robust link position controller with the direct sliding-mode joint torque controller. In Section 4, the joint torque controller based on the sliding-mode estimator is cascaded with the robust link position controller. All these control approaches take joint torque as interface variable (or better to say as state variable); thus, the extension to the end-effector force and impedance control will be straightforward. However, the singular perturbation approach does not possess joint torque tracking control capability; instead, the required joint torque for the slow dynamics (i.e., the dynamics about the link position) is implemented in a way of open-loop control, or called feedforward control. Because the singular perturbation approach is a simple and effective control approach, thus it is considered here as an alternative to the proposed controllers.

2. Singular Perturbation Approach

The composite control structure of singular perturbation approach for the slow and fast dynamics will be summarized as follows.

The robust link position controller for rigid-body manipulators is now taken as the controller for the slow dynamics of the flexible-joint robots:

$$\begin{cases} \tau_0 = M_0(q)\left(\ddot{q}_d - K_D\dot{q}_e - K_P q_e\right) + N_0(q,\dot{q}), \\ s = \dot{q}_e + K_D q_e + K_P \int_0^t q_e(\xi)\mathrm{d}\xi - \dot{q}_e(0) - K_D q_e(0) \\ \quad + \int_0^t M_0^{-1}(q)\left(\tau_1 - \tau_{1av}\right)\mathrm{d}\xi \\ \tau_1 = -\Gamma_0 \dfrac{s}{\|s\|}, \\ \tau_{1av} = \mathrm{lowpass}\left(\tau_1\right), \\ \tau_d = \tau_0 + \tau_{1av}, \end{cases} \tag{2}$$

where $M_0(q) = M(q) - \Delta M$ and $N_0(q,\dot{q}) = N(q,\dot{q}) - \Delta N$, with ΔM and ΔN being the unknown part of matrix $M(q)$ and vector $N(q,\dot{q})$, respectively; $q_e = q - q_d$ is the link position error vector; $K_D \in R^{n\times n}$ and $K_P \in R^{n\times n}$ are positive definite diagonal gain matrices determining the closed-loop performance; τ_0 represents the computed torque part of the controller; Γ_0 is a positive constant (control gain may also take other forms), and $\|s\|$ denotes the norm 2 of s, i.e., $\|s\| = \sqrt{s_1^2 + s_2^2 + \ldots + s_n^2}$; and control term τ_{1av} serves here as a perturbation compensator. The output of this controller τ_d is quasicontinuous, which is the reference input for the joint torque implementation. Normally, when using singular perturbation approach, the joint inertia matrix J has to be considered in the link position controller by adding matrix J to the mass matrix of the robot arm $M(q)$. However, since our link position controller is a robust controller, implying that no exact parameters are required, the information about the joint inertia is normally not necessary (the system robustness depends on the available control resource).

The reference current vector for the most inner current control loop can be calculated from the torque commands for the slow and fast dynamics, i.e., $\tau_{\mathrm{slow}} \in R^n$ and $\tau_{\mathrm{fast}} \in R^n$:

$$I_q^* = K_t^{-1}\tau_m = K_t^{-1}\Gamma^{-1}\left(\tau_{\mathrm{slow}} + \tau_{\mathrm{fast}}\right), \tag{3}$$

where K_t is the diagonal torque constant matrix of the electric motors and Γ is the diagonal gear-ratio matrix; $I_q^* = [i_{qi}^*] \in R^n$, $i = 1\sim n$, is the reference current vector including the reference q-axis currents for all joints; τ_m represents the motor torque vector. The slow and fast joint torque commands can be given as (taken from reference [15])

$$\begin{cases} \tau_{\mathrm{slow}} = \tau_d, \\ \tau_{\mathrm{fast}} = -D_{\mathrm{SPB}}\dot{\tau}, \\ \text{or } \tau_{\mathrm{fast}} = -K_{\mathrm{SPB}}\left(\tau - \tau_d\right) - D_{\mathrm{SPB}}\dot{\tau}, \end{cases} \tag{4}$$

with $D_{\mathrm{SPB}} \in R^{n\times n}$ and $K_{\mathrm{SPB}} \in R^{n\times n}$ being constant diagonal gain matrices to be determined by the control designer (if joint stiffness is changed, these control gain matrices need to be retuned accordingly).

For the motor current control, the equations of the current controller are written as follows (note that this current controller is only for the control of i^{th} joint motor, and the subscript i is not used for simplicity):

$$\begin{cases} s_d = i_d - i_d^*, \\ s_q = i_q - i_q^*, \\ \Omega_1 = \left(s_d\cos\theta_a - s_q\sin\theta_a\right), \\ \Omega_2 = \left(s_d\cos\theta_b - s_q\sin\theta_b\right), \\ \Omega_3 = \left(s_d\cos\theta_c - s_q\sin\theta_c\right), \\ u_1 = -u_0\,\mathrm{sign}\left(\Omega_1\right), \\ u_2 = -u_0\,\mathrm{sign}\left(\Omega_2\right), \\ u_3 = -u_0\,\mathrm{sign}\left(\Omega_3\right), \end{cases} \tag{5}$$

with i_d and i_q are the stator currents in the (d, q) coordinate frame; i_q^* is one of the components of compose controller (3); and reference current component $i_d^* = 0$ for constant torque operation and $i_d^* \neq 0$ for field-weakening operation $\theta_a = \theta_e, \theta_b = \theta_e - (2\pi/3), \theta_c = \theta_e + (2\pi/3)$, and θ_e being the rotor electrical angle of the PMSM used. This current controller does not need the motor parameters as well as the decoupling process; thus, it is a robust current controller.

From equations (2)~(5), it can be recognized that this link position control system needs very few information from the controlled plant. This is the main advantage of this control approach. The disadvantage is that the joint torque dynamics are not really controlled, but taken as disturbance and rejected by a damping term. From theory point of view and verified by the simulation studies given later, this control system is not robust with respect to the large change in the joint stiffness.

3. Extended-Regular-Form Approach

In this section, we will combine the state-space joint torque controller using direct sliding-mode control with the robust link position controller for rigid-body manipulators to form a robust link position controller for flexible-joint robots. To achieve this design goal, we need some theoretical supports.

Two methods are often used in the control of nonlinear high-order uncertain systems:

(1) The order reduction method, e.g., using singular perturbation theory

(2) The pure cascaded control method

The first method may possess a relative higher bandwidth than the pure cascaded control method, but the neglected high-frequency dynamics in the real controlled plant may be excited if high control gains are used (high control gains are often required by some robust control approaches); thus, the bandwidth will be limited in turns. The cascaded control method has the advantages: the control system is easier being set into operation and the state

variables used by the controller are measurable by some sensors. However, the bandwidth of the control system is limited by the cascaded control structure. Theoretically, the state-space control structure based on the full-state feedback has a higher control performance (i.e., higher bandwidth). However, the state-space method may need the high-order time derivatives of the sensor signal, which are difficult to obtain, because

(1) the sensor signal has always some noise

(2) a low-pass filter would introduce some time delay

(3) an observer would need a dynamic model and associated parameters

As a result, one has to do some tradeoffs. In Section 1, we have presented the three-block formulation of the flexible-joint robots. Actually, we had combined blocks B and C to control the joint torque in a way of state-space control. Moreover, because we used the direct sliding-mode control approach to implement the joint torque tracking control by applying the discontinuous terminal voltages of the motor windings directly, the joint torque controller is free from the chattering problem and is of a high robustness with respect to the system uncertainties. This control performance can hardly be achieved by a normal cascaded control structure.

For the link position control problem for flexible-joint robots dealt with in this section, we will use the state-space joint torque controller as the inner control loop. As the outer position control loop, it is nature to use the robust link position controller for rigid-body manipulators. As a result, there are totally two control loops instead of three. Because the dynamics of blocks A and $B+C$ in Figure 2 are interconnected, if we cascade the link position controller with the joint torque controller, we need associated theoretical support. For this purpose, we extend the so-called regular-form approach in the context of sliding-mode control theory.

For a general nonlinear affine system,

$$\dot{x} = f(x) + B(x)u, \tag{6}$$

where x, $f(x) \in R^n$, $B(x) \in R^{n\times m}$, and $u(x) \in R^m$, and we propose now the concept of extended-regular-form. System (6) can be rearranged or transferred to the following two-block system (see [23] for such kind of transformation, but in case of flexible-joint robots, the system equations are already in this form):

$$\begin{cases} \dot{x}_1 = f_1(x_1, x_2), \\ \dot{x}_2 = f_2(x_1, x_2) + B_2(x_1, x_2)u, \end{cases} \tag{7}$$

where $x_1 \in R^{n-l}$, $x_2 \in R^l$, and B_2 is an $l \times m$ matrix with $l \geq m$. The first block does not depend on control.

Note that the classical regular-form approach requires that the dimension of x_2 should be equal to the dimension of the control input, i.e., $l = m$, see [27]. Now, we extend this design concept to the case of $l \geq m$.

The control design is performed in two stages. At first, the l-dimensional state vector x_2 is handled as the control input for the first block and designed as a function of the state vector x_1 of the first block according to some performance criteria:

$$x_2^d = -s_0(x_1). \tag{8}$$

Then, for the control of x_2 in the second block to be equal to the one given above, we design the control u using the sliding-mode control theory to achieve the required robustness with respect to the system uncertainties including the influence of x_1 to the second block, so now we deal with a reduced order problem of an uncertain system. At this second stage, discontinuous control u is to be designed to enforce sliding mode in the manifold:

$$s = C\left(x_2 - x_2^d\right) = 0, \tag{9}$$

where $C \in R^{m\times l}$ is a designed constant matrix determining the system behavior in sliding mode (note that s may also take other forms). In sliding mode, the system motion is governed by

$$\begin{cases} \dot{x}_1 = f_1(x_1, x_2), \\ C\left(x_2 - x_2^d\right) = 0. \end{cases} \tag{10}$$

The second system in (6)–(10) is of $l - m$ order, the convergence of x_2 to x_2^d depends only on the designed parameter matrix C, and theoretically, the poles of the second system can be placed arbitrarily, implying that the system response can be designed as fast as required. Therefore, a fast convergence of x_2 to x_2^d can be achieved by properly selecting matrix C (under the condition that the sliding mode already occurs). If the control gains used in controller (8) are not infinitely high, the motion in (10) can be classified into slow and fast dynamics (corresponding to the first and second equation of (10), respectively). Depending on singular perturbation theory, for the slow dynamics, i.e., the first equation of (10) $x_2 = x_2^d$ can be assumed. As a result, the slow dynamics will be stabilized by the feedback control given in (8) and the following final system will be stable as expected:

$$\dot{x}_1 = f_1(x_1, -s(x_1)). \tag{11}$$

For the control of flexible-joint robots, x_1 in (7) stands for the state vector of the link position system (which is a second-order system) and x_2 presents the state vector of the joint torque system (which is a third-order system including the dynamics of motor current).

As mentioned before, we intend to use the link position controller to control the link position and to use the joint torque controller to control the joint torque. Both controllers are robust controller based on sliding-mode technique. The joint torque controller utilizes the switching property of the power converter (i.e., the inverter), implying that we are not suffered from the chattering problem.

3.1. Link Position Controller of the Robot Arm. The controller algorithm for this section can be summarized as follows:

$$\begin{cases} \tau_0 = M_0(q)\left(\ddot{q}_d - K_D\dot{q}_e - K_P q_e\right) + N_0(q,\dot{q}), \\ s = \dot{q}_e + K_D q_e + K_P \int_0^t q_e(\xi)\mathrm{d}\xi - \dot{q}_e(0) - K_D q_e(0) \\ \quad + \int_0^t M_0^{-1}(q)\left(\tau_1 - \tau_{1av}\right)\mathrm{d}\xi, \\ \tau_1 = -\Gamma_0 \dfrac{s}{\|s\|}, \\ \tau_{1av} = \mathrm{lowpass}\left(\tau_1\right), \\ \tau_d = \tau_0 + \tau_{1av}. \end{cases} \tag{12}$$

See Section 2 for the definitions of variables and parameters as equation (2).

3.2. Joint Torque Controller of i^{th} Robot Joint (Subscript i Is Not Used for Simplicity).

$$\begin{cases} e_\tau = \tau - \tau_d, \\ s_\tau = e_\tau + c_1\dot{e}_\tau + c_0 e_\tau, \\ s_d = A^{-1}L\left(i_d - i_d^*\right), \\ \Omega_1 = \left(s_d\cos\theta_a - s_\tau\sin\theta_a\right), \\ \Omega_2 = \left(s_d\cos\theta_b - s_\tau\sin\theta_b\right), \\ \Omega_3 = \left(s_d\cos\theta_c - s_\tau\sin\theta_c\right), \\ u_1 = -u_0\,\mathrm{sign}\left(\Omega_1\right), \\ u_2 = -u_0\,\mathrm{sign}\left(\Omega_2\right), \\ u_3 = -u_0\,\mathrm{sign}\left(\Omega_3\right), \end{cases} \tag{13}$$

where $e_\tau = \tau - \tau_d$ is the joint torque control error. The parameter $A^{-1}L = k\gamma k_t/J$ is introduced in s_d to simplify the control design; the parameters c_0 and c_1 have to be provided by the control designer depending on the required closed-loop performance of the joint torque control. The definitions of other variables and parameters in the control system are given by (12) and (13), see Section 2.

4. Cascaded Control Structure Based on the Sliding-Mode Estimator Approach

In this section, we use the joint torque controller for the inner torque control loop and the robust link position controller for the outer link position control loop. This combination has an advantage comparing to the approach given in the previous section, namely, signal τ is not required. However, it has also some disadvantages:

(1) The control algorithm needs the nominal value of some parameters

(2) The joint torque control performance for large or fast changing reference torques is not as good as the one of direct sliding-mode control approach

(3) It needs an inner current control loop for the control of i_q; thus, there are totally three control loops instead of two.

4.1. Link Position Controller of the Robot Arm. The controller algorithm for this section can be summarized as follows:

$$\begin{cases} \tau_0 = M_0(q)\left(q_d - K_D\dot{q}_e - K_P q_e\right) + N_0(q,\dot{q}), \\ s = \dot{q}_e + K_D q_e + K_P \int_0^t q_e(\xi)\mathrm{d}\xi - \dot{q}_e(0) - K_D q_e(0) \\ \quad + \int_0^t M_0^{-1}(q)\left(\tau_1 - \tau_{1av}\right)\mathrm{d}\xi, \\ \tau_1 = -\Gamma_0 \dfrac{s}{\|s\|}, \\ \tau_{1av} = \mathrm{lowpass}\left(\tau_1\right), \\ \tau_d = \tau_0 + \tau_{1av}. \end{cases} \tag{14}$$

See Section 2 for the definitions of variables and parameters as equation (2).

4.2. Joint Torque Controller of i^{th} Robot Joint (Subscript i Is Not Used for Simplicity).

$$\begin{cases} e_\tau = \tau - \tau_d, \\ \tau_f = \widehat{b}^{-1}\left(\widehat{a}\tau + \tau_d - c_1\dot{e}_\tau - c_0 e_\tau\right), \\ \widehat{z}(0) = \dot{\tau}(0), \\ u_{eq} = \mathrm{lowpass}\left(M_s\,\mathrm{sign}\left(\widehat{z} - \dot{\tau}\right)\right), \\ \tau_r = \widehat{b}^{-1}u_{eq}, \\ \dot{\widehat{z}} = \tau_d - c_1\dot{e}_\tau - c_0 e_\tau + \widehat{b}\tau_r - M_s\,\mathrm{sign}\left(\widehat{z} - \dot{\tau}\right), \\ \tau_m = \tau_f + \tau_r, \end{cases} \tag{15}$$

where $\widehat{z}$ is the artificially introduced auxiliary variable, which is actually an estimate of $\dot{\tau}$. Parameters $\widehat{a}$, $\widehat{b}$, c_0, c_1, and M_s, and the time constant of the low-pass filter have to be provided by the control designer. The definitions of others variables and parameters are given in Section 2. The stability proof of controller (15) is similar to the literature [28].

A current controller for the control of i_q is required as the most internal control loop (the same happens with the control system presented in Section 2). The current controller used here could be the same as the one given by

equation system (5) (sure, a classical current controller with conventional PWM may be employed too).

5. Simulation Studies

5.1. Plant Model Used for the Simulation. To verify the proposed control approaches, we use a two-link flexible-joint robot as the plant model shown in Figure 3, which consists of the two-link rigid-body robot model which can be given as

$$\begin{bmatrix} m_{11} & m_{12} \\ m_{21} & m_{22} \end{bmatrix} \begin{bmatrix} \ddot{q}_1 \\ \ddot{q}_2 \end{bmatrix} + \begin{bmatrix} d_1 + g_1 + f_1 \\ d_2 + g_2 + f_2 \end{bmatrix} = \begin{bmatrix} \tau_1 \\ \tau_2 \end{bmatrix},$$

$$\text{ie. } M(q) = \begin{bmatrix} m_{11} & m_{12} \\ m_{21} & m_{22} \end{bmatrix},$$

$$N(q, \dot{q}) = \begin{bmatrix} d_1 + g_1 + f_1 \\ d_2 + g_2 + f_2 \end{bmatrix}, \tag{16}$$

with

$$\begin{aligned} m_{22} &= L_2^2 M_2, \\ m_{12} &= m_{21} = m_{22} + L_1 L_2 M_2 \cos q_2, \\ m_{11} &= L_1^2 (M_1 + M_2) + 2m_{12} - m_{22}, \\ d_1 &= -L_1 L_2 M_2 \left(2\dot{q}_1 \dot{q}_2 - \dot{q}_2^2\right) \sin q_2, \\ d_2 &= L_1 L_2 M_2 \dot{q}_1^2 \sin q_2, \\ g_2 &= L_2 M_2 g \cos(q_1 + q_2), \\ g_1 &= L_1 (M_1 + M_2) g \cos(q_1) + g_2, \\ f_1 &= k_{v1} \dot{q}_1 + k_{c1} \operatorname{sign}(\dot{q}_1), \\ f_2 &= k_{v2} \dot{q}_2 + k_{c2} \operatorname{sign}(\dot{q}_2). \end{aligned} \tag{17}$$

The parameters of the two-link flexible-joint robot used for the simulation are listed in Tables 1~3.

5.2. Reference Input for Testing the Link Position Controllers. For the link position tracking control, we demand the manipulator to move along a circular trajectory in its workspace; see the following equation:

$$\begin{cases} x_d(t) = x_{d0} + r_d \cos \psi_d, \\ y_d(t) = y_{d0} - r_d \sin \psi_d, \\ \psi_d(t) = \dfrac{2\pi}{t_f} t - \sin\left(\dfrac{2\pi}{t_f} t\right), \\ 0 \le t \le t_f. \end{cases} \tag{18}$$

The parameters of the circle are given as $r_d = 1.0$ m, $x_{d0} = 0.5$ m, and $y_{d0} = 0.5$ m. The simulation time is now selected as $t_f = 4$ s in order to zoom-in the transition period. Through the inverse kinematics, the reference link positions

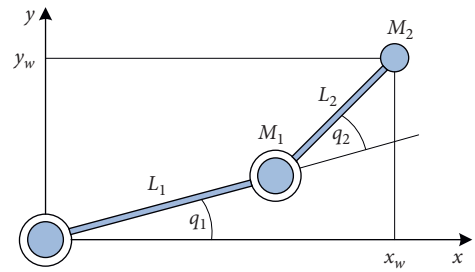

Figure 3: Two-link manipulator with link lengths L_1 and L_2 and concentrated link masses M_1 and M_2 (the manipulator is shown in joint configuration (q_1, q_2), which leads to end-effector position (x_w, y_w) in world coordinates).

Table 1: Arm parameters.

M_1	M_2	L_1	L_2
4 kg	2 kg	0.5 m	0.5 m

Table 2: Parameters for motor1 and motor2.

$L(H)$	R(Ohm)	λ_0	P	k_t (Nm/A)	$I_{q\_\max}$ (A)	U_0 (V)
44.5×10^3	0.68	0.24	4	$(3/2)P\lambda_0$	60	120

Table 3: Parameters of joint 1 and joint 2.

J (kgm^2)	k (Nm/Rad)	γ	k_ω (Nm/(Rad/s))
1.5	10000	40	1

for joint 1 and joint 2 are calculated according to equation (19). This reference trajectory will generate large and fast changing joint torques to be followed:

$$\begin{cases} q_2 = a\tan 2(D, C), \text{ with } C = \dfrac{x_w^2 + y_w^2 - L_1^2 - L_2^2}{2L_1 L_2}, \\ D = \pm \sqrt{1 - C^2}, \\ q_1 = a\tan 2(y_w, x_w) - 2a\tan 2\left(L_2 \sin q_2, L_1 + L_2 \cos q_2\right). \end{cases} \tag{19}$$

5.3. Controller Parameters. The parameters for the outer position control loop of Sections 2~4 are selected to be the same, and they are

$$\begin{aligned} M_0(q) &= \begin{bmatrix} 2.0 & 0 \\ 0 & 1 \end{bmatrix}, \\ N_0(q, \dot{q}) &= \begin{bmatrix} 0 \\ 0 \end{bmatrix}, \\ K_p &= \begin{bmatrix} 120 & 0 \\ 0 & 120 \end{bmatrix}, \\ K_d &= \begin{bmatrix} 50 & 0 \\ 0 & 50 \end{bmatrix}, \\ \Gamma_0 &= \begin{bmatrix} 200 & 0 \\ 0 & 200 \end{bmatrix}. \end{aligned} \tag{20}$$

The joint torques of both joints are limited to 200 Nm. The time constant of the two low-pass filters to extract the equivalent control of $\tau_1 \in R^2$ is 0.01 s. To improve the control performance, this time constant is linearly increased from zero to 0.01 s in the first half second and remains constant thereafter, similar to the following equation:

$$u(t) = \begin{cases} \left(\dfrac{0.025}{0.5}\right)t, & 0 \le t \le 0.5, \\ 0.025, & t > 0.5. \end{cases} \tag{21}$$

For the singular perturbation approach described in Section 2, the simple form fast $\tau_{\text{fast}} = -D_{\text{SPB}}\dot{\tau}$ is used for the fast dynamics, where matrix D_{SPB} is selected as

$$D_{\text{SPB}} = \begin{bmatrix} 0.002 & 0 \\ 0 & 0.002 \end{bmatrix}. \tag{22}$$

For the extended-regular-form approach described in Section 3, the inner loop joint torque controller parameters are selected to be the same as those given by

$$\begin{cases} c_{01} = 20000, \\ c_{11} = 200, \\ \left(A^{-1}L\right)_1 = 3.84 \times 10^5, \\ c_{02} = 20000, \\ c_{12} = 200, \\ \left(A^{-1}L\right)_2 = 3.84 \times 10^5. \end{cases} \tag{23}$$

For the cascaded control structure based on the sliding-mode estimator approach described in Section 4, the inner loop joint torque controller parameters are the same as those given by

$$\begin{cases} J_{m1\_n} = \dfrac{1.3J_1}{\gamma_1^2}, \\ J_{l1\_n} = 1.5m_{11|q_2=0} = 1.5\left(L_1^2M_1 + (L_1 + L_2)^2M_2\right), \\ k_{1\_n} = 0.5k_1, \\ J_{m2\_n} = \dfrac{1.3J_2}{\gamma_2^2}, \\ J_{l2\_n} = 1.5m_2 = 1.5L_2^2M_2, \\ k_{2\_n} = 0.5k_2, \end{cases}$$

$$\begin{cases} \widehat{a}_1 = \dfrac{k_{1\_n}}{\gamma_1^2 J_{m1\_n}} + \dfrac{k_{1\_n}}{J_{l1\_n}}, \\ \widehat{b}_1 = \dfrac{k_{1\_n}}{\gamma_1^2 J_{m1\_n}}, \\ \widehat{a}_2 = \dfrac{k_{2\_n}}{\gamma_2^2 J_{m2\_n}} + \dfrac{k_{2\_n}}{J_{l2\_n}}, \\ \widehat{b}_2 = \dfrac{k_{2\_n}}{\gamma_2^2 J_{m2\_n}}, \end{cases}$$

$$\begin{cases} c_{01} = 20000, \\ c_{11} = 200, \\ M_{s1} = 2 \times 10^6, \\ \mu_1 = 1 \times 10^{-3}, \\ c_{02} = 20000, \\ c_{12} = 200, \\ M_{s2} = 2 \times 10^6, \\ \mu_2 = 1 \times 10^{-3}. \end{cases} \tag{24}$$

5.4. Simulation Results and Discussion. Figures 4~8 show the simulation results of the link position tracking control of the two-joint robot arm considering the joint flexibility and the AC-motor dynamics. Figures 4 and 5 are for the case of normal joint stiffness, i.e., $k_1 = k_2 = 10000$ Nm/Rad; while Figures 6 and 7 are for the case of large joint compliance, i.e., very small joint stiffness $k_1 = k_2 = 1000$ Nm/Rad (without changing the controller parameters).

As one can see from Figures 4 and 5, for the normal joint stiffness (i.e., $k_1 = k_2 = 10000$ Nm/Rad), the singular perturbation approach and two new presented control approaches given in Sections 2~4 have similar tracking control performance. However, for the case of large joint compliance ($k_1 = k_2 = 1000$ Nm/Rad), see Figures 6 and 7, the singular perturbation approach shows a poorer control performance, due to the lack of adaptation mechanisms to the changing of the joint stiffness. The extended-regular-form approach based on the direct sliding-mode joint torque control and the cascaded control structure based on the sliding-mode estimator (for joint torque control) show similar control performance for the normal and the small joint stiffness at first glance. However, if we take a close look in the joint torque tracking performance in the inner control loop (see Figure 8 for the joint torque tracking of joint 1 in zoomed time range of 1s), it can be found immediately that the direct sliding-mode joint torque controller under the extended-regular-form approach has a much better tracking performance as the one of the sliding-mode estimator approach under the cascaded control structure. This result confirms the theoretical expectation.

Actually, a simple high-gain controller is not adequately being used within a cascaded multiple-loop control system, except for the most internal control loop. This is the reason why we tried to reduce the number of control loops and use the sliding-mode (i.e., high gain) controller in the most internal control loop, as done with the extended-regular-form approach.

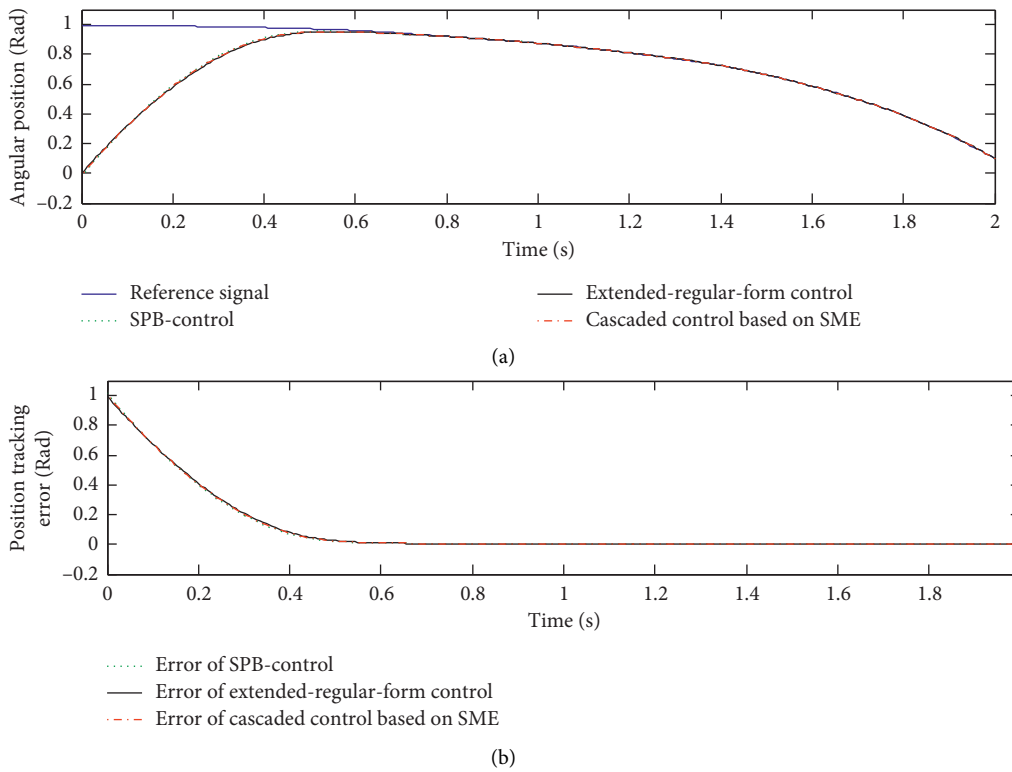

Figure 4: Position control of joint 1 (normal joint stiffness). (a) Angular position tracking of joint 1. (b) Position tracking error of joint 1.

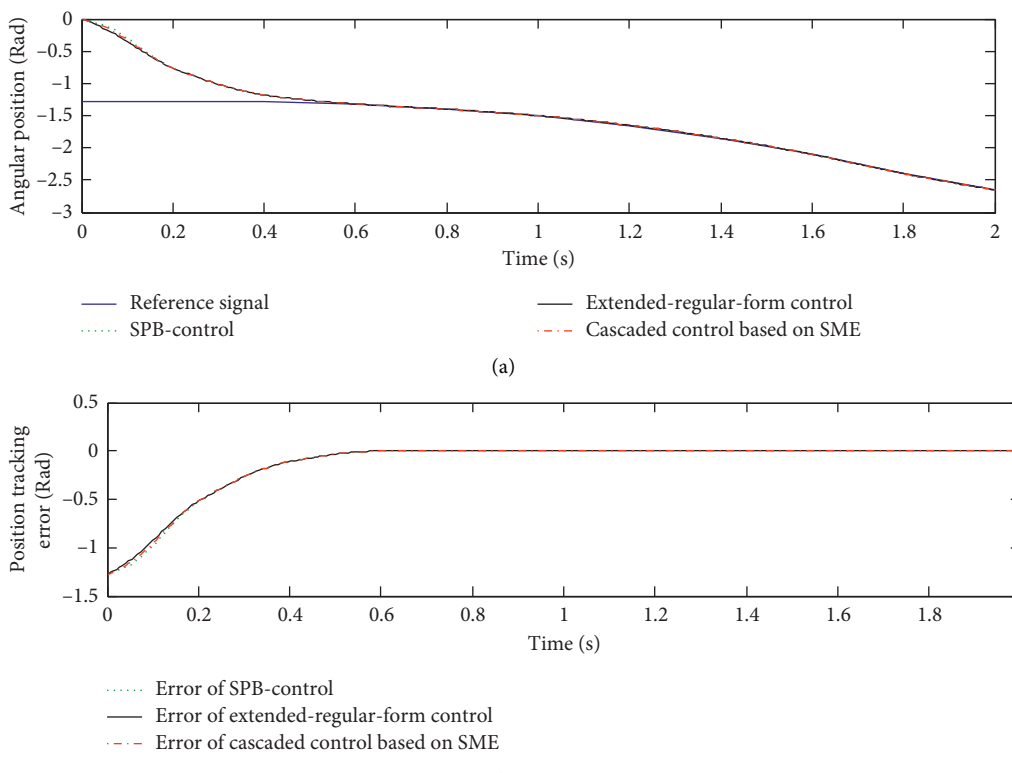

Figure 5: Position control of joint 2 (normal joint stiffness). (a) Angular position tracking of joint 2. (b) Position tracking error of joint 2.

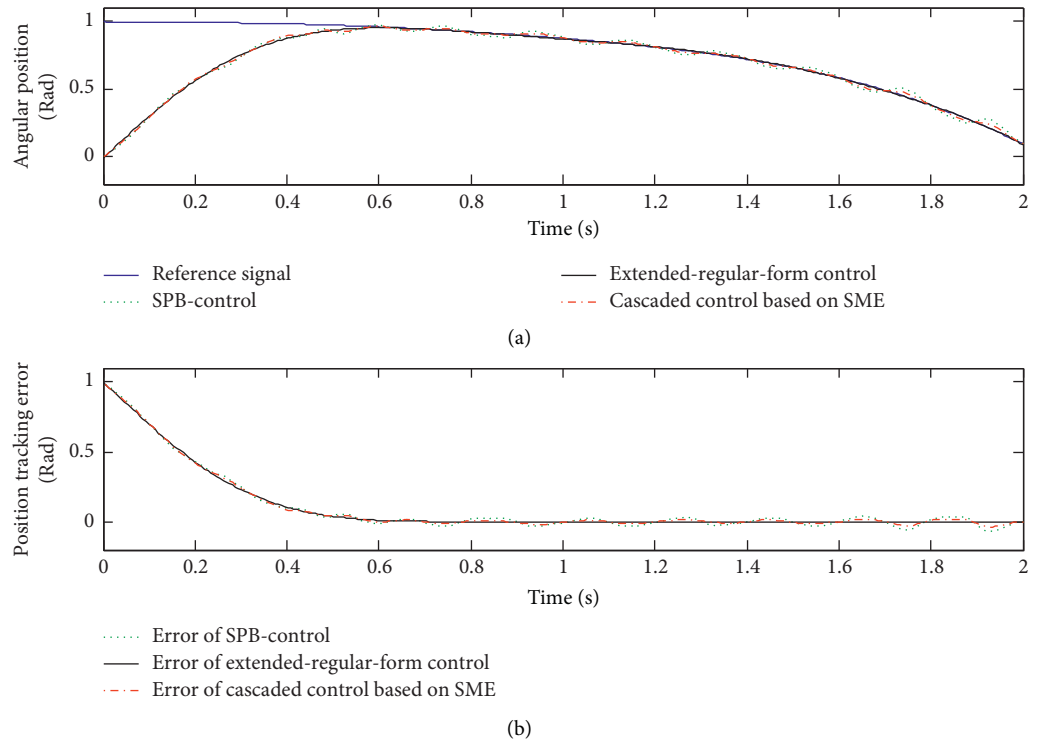

Figure 6: Position control of joint 1 (large joint compliance). (a) Angular position tracking of joint 1. (b) Position tracking error of joint 1.

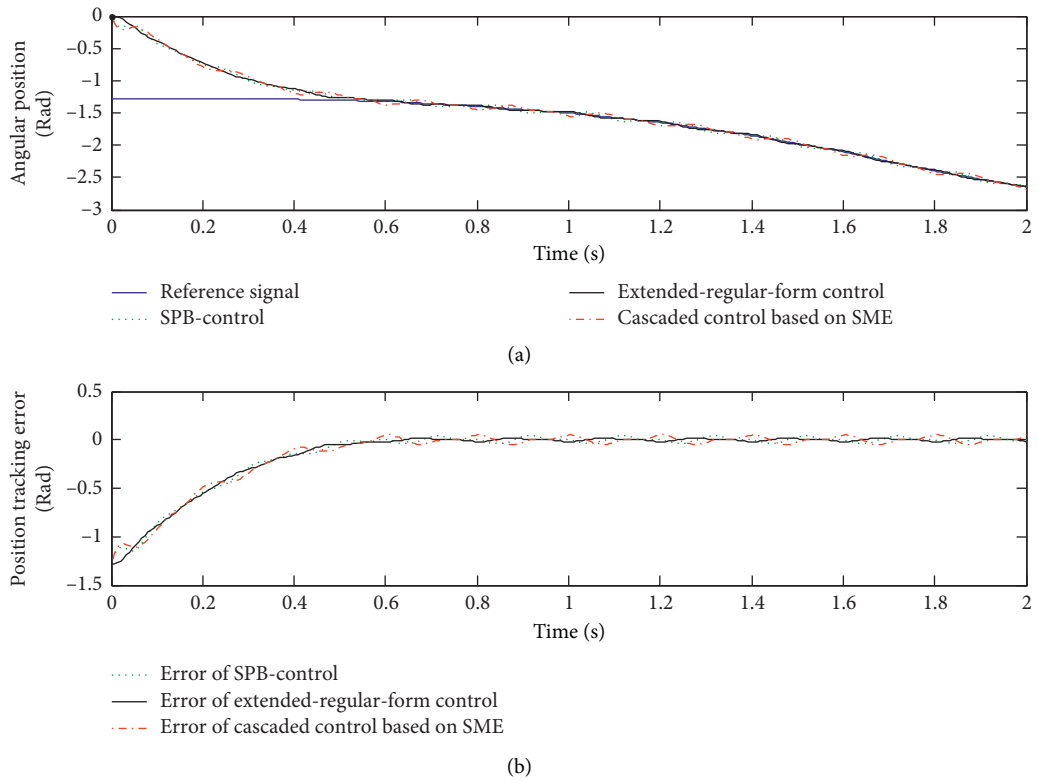

Figure 7: Position control of joint 2 (large joint compliance). (a) Angular position tracking of joint 2. (b) Position tracking error of joint 2.

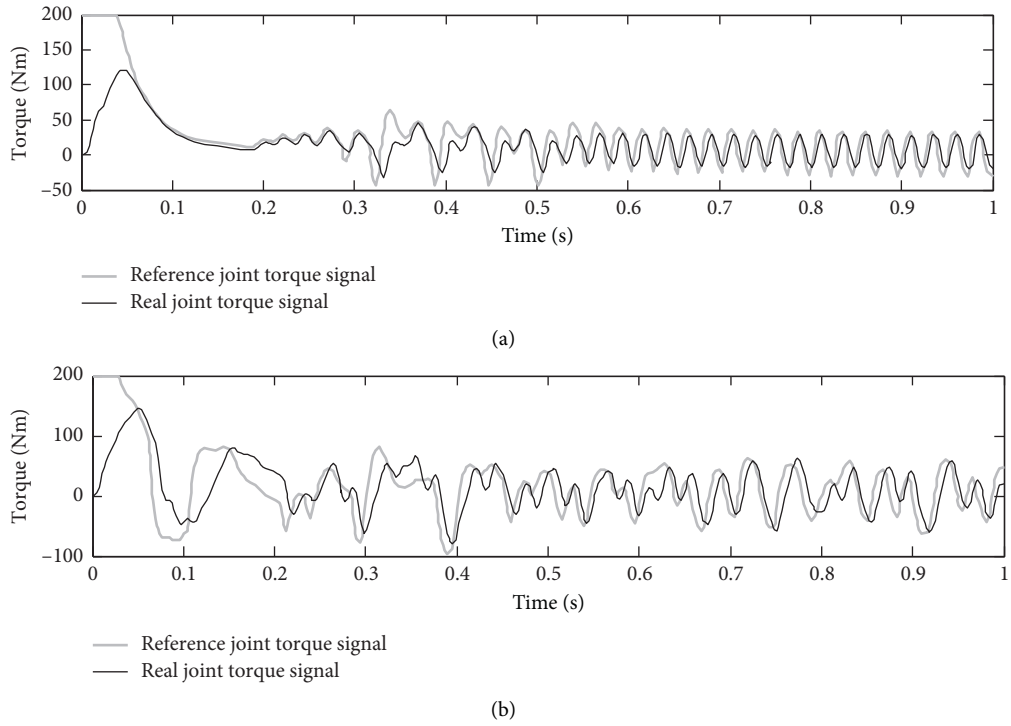

Figure 8: Joint torque tracking control of joint 1 (large joint compliance). (a) Inner loop joint torque control by direct sliding-mode control. (b) Inner loop joint torque control by sliding-mode estimator (grey solid line = reference joint torque signal; black solid line = real joint torque signal).

6. Conclusions

In this paper, the three-block formulation of the dynamics for flexible-joint robots was introduced at first. Then, singular perturbation approach and two new control approaches are presented for the link position tracking control of this kind of robot. Among them, the singular perturbation approach (famous approach) is the simplest one for the real-time implementation, but it is sensitive to the changing of joint stiffness, from a theory point of view and verified by the simulation studies. The extended-regular-form approach with the direct sliding-mode joint torque control has the highest control performance, and the implementation is also quite simple, except for the requirement on the second-time derivative of the joint torque signal. The cascaded control structure based on the sliding-mode estimator approach tries to avoid the second-time derivative of the joint torque signal but possesses a more involved control structure and needs more controller parameters than the other two.

These comparative studies confirm again that there is no free lunch in the control of high-order uncertain systems, unless to give up the intention of achieving high bandwidth. The proposed extended-regular-form concept can also be applied to some other high-order, nonlinear, uncertain systems.

Moreover, there are still some topics left which need to be investigated in the future research works. One is achieving a usable second-time derivative of noisy joint torque signal with minimal time delay and, at the same time, reducing the sensitivity of the control algorithms with respect to the noisy joint torque signal. The other is seeking the hardware solution for the direct sliding-mode joint torque control (without using the build-in PWM in microcontrollers or DSP) to achieve the advanced control performances provided by this control approach.

Data Availability

The RAR data used to support the findings of this study are included within the supplementary information file.

Additional Points

The concept of extended-regular-form for the block-control of high-order uncertain systems is proposed. The proposed method breaks through the limitation (under certain given condition) that the dimension of the inner block must be equal to the dimension of the control input associated with the conventional regular-form approach. The proposed method serves as the theoretical support for cascading an outer position control loop with the inner direct (state-space) sliding-mode joint torque control loop for the trajectory tracking control of flexible-joint robots.

Conflicts of Interest

The authors declare that they have no conflicts of interest.

Acknowledgments

This project was supported by the National Natural Science Foundation of China (NSFC, nos. 61763030 and 61263045), the Jiangxi Province Science and Technology Support Project (20112BB550017), and the Jiangxi Province Natural Science Fund Project (20132BAB201040).

Supplementary Materials

Supplementary materials are simulation experiment data results and responses to reviewers, and these data are mainly for Figures 4–8. (*Supplementary Materials*)

References

[1] M. W. Spong, "Modeling and control of elastic joint robots," *The Journal of Dynamic Systems, Measurement, and Control*, vol. 109, no. 4, pp. 310–318, 1987.

[2] M. W. Spong, "Modeling and control of elastic joint robots," *IEEE Journal of Robotics and Automation*, vol. 3, no. 4, pp. 291–300, 1987.

[3] L. Le-Tien and A. Albu-Schaffer, "Robust adaptive tracking control based on state feedback controller with integrator terms for elastic joint robots with uncertain parameters," *IEEE Transactions on Control Systems Technology*, vol. 26, no. 6, pp. 2259–2267, 2018.

[4] A. De Luca and L. Lanari, "Robots with elastic joints are linearizable via dynamic feedback," in *Proceedings of 34th IEEE Conference on Decision and Control*, pp. 3895–3897, New Orleans, LA, USA, December 1995.

[5] A. De Luca and P. Lucibello, "A general algorithm for dynamic feedback linearization of robots with elastic joints," in *Proceedings of the IEEE International Conference of Robotics and Automation*, pp. 504–510, Leuven, Belgium, May 1998.

[6] S. E. Talole and S. B. Phadke, "Extended State Observer Based Control of Flexible Joint System," in *Prooceedings of the IEEE International Symposium on Industrial Electronics*, pp. 2514–2519, Cambridge, UK, June 2008.

[7] S. E. Talole, J. P. Kolhe, and S. B. Phadke, "Extended-state-observer-based control of flexible-joint system with experimental validation," *IEEE Transactions on Industrial Electronics*, vol. 57, no. 4, pp. 1411–1419, 2010.

[8] M. C. Readman, *Flexible Joint Robots*, CRC Press, Boca Raton, FL, USA, 1994.

[9] Z. Shao and X. Zhang, "Intelligent control of flexible-joint manipulator based on singular perturbation," in *Proceedings of the IEEE International Conference on Automation and Logistics*, pp. 243–248, Hong Kong, China, August 2010.

[10] M. A. Khosravi and H. D. Taghirad, "Dynamic modeling and control of parallel robots with elastic cables: singular perturbation approach," *IEEE Transactions on Robotics*, vol. 30, no. 3, pp. 294–704, 2014.

[11] A. Izadbakhsh and M. Masoumi, "FAT-based robust adaptive control of flexible-joint robots: singular perturbation approach," in *Proceedings of the IEEE International Conference on Industrial Technology (ICIT)*, pp. 22–25, Toronto, ON, Canada, March 2017.

[12] J. Kim and E. A. Croft, "Full-state tracking control for flexible joint robots with singular perturbation techniques," *IEEE Transactions on Control Systems Technology*, vol. 27, no. 1, pp. 63–73, 2019.

[13] L. Zouari, H. Abid, and M. Abid, "Backstepping controller for electrically driven flexible joint manipulator under uncertainties," *International Journal of Applied Engineering Research*, vol. 10, no. 8, pp. 19885–19896, 2015.

[14] Z. H. Jiang and K. Shinohara, "Workspace trajectory tracking control of flexible joint robots based on backstepping method," in *Proceedings of the IEEE Region 10 Conference (TENCON)*, pp. 3473–3476, Singapore, November 2016.

[15] C. Ott, *Cartesian Impedance Control of Redundant and Flexible-Joint Robots*, Springer, Berlin, Germany, 2008.

[16] C. Schindlbeck and S. Haddadin, "Unified passivity-based cartesian force/impedance control for rigid and flexible joint robots via task-energy tanks," in *Proceedings of the IEEE International Conference on Robotics and Automation*, pp. 440–447, Seattle, WC, USA, May 2015.

[17] R. Reyes-Báez and A. J. van der Schaft, "Virtual differential passivity based control for tracking of flexible-joints robots," in *Proceedings of the Workshop on Lagrangian and Hamiltonian Methods in Nonlinear Control*, pp. 1–8, Nagoya, Japan, July 2017.

[18] V. I. Utkin, J. Guldner, and J. Shi, *Sliding Mode Control in Electromechanical Systems*, Taylor & Francis publisher, Oxfordshire, UK, Second edition, 2009.

[19] S. Kwon, A. Asignacion, and S. Park, "Control of flexible joint robot using integral sliding mode and backstepping," *Automation, Control and Intelligent Systems*, vol. 4, no. 6, pp. 95–100, 2016.

[20] S. Mobayen and F. Tchier, "Nonsingular fast terminal sliding-mode stabilizer for a class of uncertain nonlinear systems based on disturbance observer," *Scientia Iranica*, vol. 24, no. 3, pp. 1410–1418, 2017.

[21] D. A. Haghighi and S. Mobayen, "Design of an adaptive super-twisting decoupled terminal sliding mode control scheme for a class of fourth-order systems," *ISA Transactions*, vol. 75, pp. 216–225, 2018.

[22] O. Mofid, S. Mobayen, and M. H. Khooban, "Sliding mode disturbance observer control based on adaptive synchronization in a class of fractional-order chaotic systems," *International Journal of Adaptive Control and Signal Processing*, vol. 33, no. 3, pp. 462–474, 2018.

[23] M. Jin, J. Lee, and T. Ng, "Model-free robust adaptive control of humanoid robots with flexible joints," *IEEE Transactions on Industrial Electronics*, vol. 64, no. 2, pp. 1706–1715, 2017.

[24] B. Farzanegan and S. D. Banadaki, "Direct artificial neural network control of single link flexible joint," in *Proceedings of the 2016 4th International Conference on Control, Instrumentation, and Automation (ICCIA)*, pp. 131–135, Qazvin, Iran, January 2016.

[25] M. J. Kim and W. K. Chung, "Disturbance-observer-based PD control of flexible joint robots for asymptotic convergence," *IEEE Transactions on Robotics*, vol. 31, no. 6, pp. 1508–1516, 2015.

[26] N. Vitiello, T. Lenzi, and S. R. SMM De Rossi, "A sensorless torque control for antagonistic driven compliant joints," *Mechatronics*, vol. 20, no. 3, pp. 355–367, 2010.

[27] A. Lukyanov and V. I. Utkin, "Methods of reducing equations for dynamic systems to a regular form," *Automation Remote Control*, vol. 42, pp. 413–420, 1981.

[28] G.-L. Xiong, H.-C. Chen, J.-X. Shi, and F.-Y. Liang, "Joint torque control of flexible joint robots based on sliding mode technique," *International Journal of Advanced Robotic Systems*, vol. 16, no. 3, pp. 1–16, 2019.